Dynamic dislocation phenomena in single crystals of Cu–10.5-at.%-Al alloys at 4.2 °K†

R. B. Schwarz* and J. W. Mitchell
Department of Physics, University of Virginia, Charlottesville, Virginia 22901
(Received 13 August 1973)

Single crystals of Cu–10.5-at.%-Al alloys with the $[\bar{1}2\bar{5}]$ $\{1\bar{2}\bar{1}\}$ $\{\bar{2}\bar{1}0\}$ orientation experience discontinuous elongations under tensile stress at 4.2 °K. The processes are initiated at a resolved shear stress of 3.01 kg mm^{-2} on the $\{\bar{1}\bar{1}1\}$ ⟨101⟩ glide system. They introduce slip bands with a mean width of 47 μm and produce a mean integrated shear displacement of 5.7 μm corresponding to the motion of 3.5×10^4 dislocations in near-edge orientations. Simultaneous elongation-time and stress-time records have been obtained with capacitive and ceramic piezoelectric transducers located near the site of relaxation in the cryostat. After an initial interval of 30 μsec, elongation proceeds at a constant rate of 1.1 cm sec^{-1} for 400 μsec. During this process, the shear stress is 0.024 kg mm^{-2} lower than at the onset of relaxation. The rate of elongation, which is determined by the mechanical properties of the system, gives a value for the product of the number and velocity of the moving dislocations of 3.76×10^7 cm sec^{-1}. Observations of the surface topography of the slip bands and of the dislocation-etch-pit distributions within them are used to establish a model for the sequence of events during the relaxation process. With this model, the mean velocity of the dislocations is found to be 2.1×10^4 cm sec^{-1} at a resolved shear stress of 2.98 kg mm^{-2} and a local steady-state temperature of 17 °K.

I. INTRODUCTION

Load-elongation records showing successive abrupt load drops have been obtained during the tensile deformation of specimens of pure metals and alloys at low temperatures in a number of investigations. Blewitt, Coltman, and Redman[1] and Blewitt, Coltman, Jamison, and Redman[2] observed discontinuous slip with Lüders-band propagation above a well-defined yield point in neutron-irradiated single crystals of copper at 4.2 °K. The load drops which involve rapid local plastic deformation have been attributed to the generation and migration of dislocations at high rates at the high stresses at which they occur.[3–5]

Basinski[6,7] studied serrated yielding at 4.2 °K in polycrystalline specimens of superpurity aluminum and 24S aluminum alloy. He attributed the discontinuous load drops to thermal instabilities. The thermal energy liberated during plastic deformation at low temperatures may cause a considerable local rise in temperature because of the low specific heat and low thermal conductivity of the specimens. Since the flow stress normally decreases with increasing temperature, the system would be unstable after the initiation of relaxation. Basinski established lower limits for the temperature increment and correlated temperature pulses with load drops by displaying signals simultaneously with a double-beam oscillograph. Similar temperature transients were recorded for polycrystalline specimens of Cu-Ni alloys by Erdmann and Jahoda.[8] Kamada,[5] Kamada, Yoshizawa, and Chihaya,[9] and Kamada and Yoshizawa,[10] studied serrated yielding at 4.2 °K and higher temperatures in single crystals of α-phase Cu-Al alloys with 1.2- to 14.2-at.% Al and also reported that such yielding is observed in single crystals of α-phase Cu-Si and Cu-Ge alloys but not in Cu-Ni alloys. Kamada rejected the thermal instability mechanism in favor of the mechanism based on rapid generation and migration of dislocations. His discussion of the thermal behavior of the crystal during deformation at 4.2 °K does not appear to be entirely valid.

There is no general agreement on the rate-determining mechanism during serrated yielding at low temperatures and either or both of the mechanisms proposed may be operative in different systems. In all of the previous work, no quantitative measurements as a function of the time of either the local elongation or of the stress at the site of relaxation have been made, and no discussion of the role of the dynamical properties of the mechanical system has been introduced.

The objectives of the present work have been to make a detailed quantitative study of the dynamical conditions governing a fast localized relaxation process at 4.2 °K in the single-crystal element of the elastically strained mechanical system and of the numbers, configurations, and average velocities of the dislocations involved in the process. No one has previously attempted to make all the observations and measurements needed to allow the macroscopic aspects of the fast-relaxation processes to be correlated with the microscopic-dislocation mechanisms responsible for them.

II. EXPERIMENTAL METHODS

A. Growth and preparation of the crystals

The methods developed for the growth of alloy crystals with large subgrains and low dislocation densities have already been described.[11] All the work presented here has been done with crystals

of the Cu–10.5-at. %-Al alloy with the $[\bar{1}2\bar{5}]\{1\bar{2}\bar{1}\}\{\bar{2}\bar{1}0\}$ orientation.[12] The alloy was produced and the crystals grown in graphite molds heated with a high-frequency induction furnace in a vacuum maintained at 2×10^{-7} Torr with a large-capacity ion pump. The as-grown dimensions were $12\times0.45\times0.45$ cm. The crystals were annealed in a closed graphite tube at a temperature 100 °C below the melting point for 100 h at a pressure of 10^{-8} Torr, also maintained with an ion pump. Sections 7.5 cm long were then chemically polished on all four surfaces.[13] To localize the relaxation processes in the center of the crystal, two shallow grooves were made in the $\{1\bar{2}\bar{1}\}$ surfaces with edges along the $\langle 101\rangle$ traces of the $\{\bar{1}\bar{1}1\}$ glide planes, a width of 4.75 mm and a depth of 0.1 mm. The surfaces were then electropolished[13] and the damage introduced by spark erosion completely removed. The final cross section was very nearly 0.43×0.43 cm, apart from the thinned section. The crystals were then mounted in a nitrogen atmosphere with Cerromatrix alloy in phosphor bronze grips which were held by the universal heads of the tensile system.

B. Tensile system and the cryostat

The detailed design of the tensile system and cryostat will be presented elsewhere. It has an outer stainless-steel tube attached through a flange to the underside of the cross-head of the Instron machine. A universal head is located at the bottom of this tube. The crystal is mounted between this head and a second universal head from which a stainless-steel pull-tube passes upwards through the cross-head to a third universal head and a steel block replacing the Instron load cell. The system was designed to minimize the reflection of stress waves at the universal head between the crystal and the stainless-steel pull tube. The crystal was cooled to 4.2 °K and the temperature was measured with a calibrated Ge thermometer mounted on the lower grip.

C. Transducer and recording systems

The details of the transducers and recording systems will be published elsewhere. For the accurate absolute measurement of the critical load required for the initiation of the abrupt elongations, and the magnitude of the associated load drops, a proving ring with a strain-gauge transducer, calibrated with standard weights, was introduced immediately below the third universal head. A higher sensitivity for the measurement of the abrupt elongations was achieved with a high-frequency differential transformer, mounted along the vertical axis of the proving ring.

The local rate of elongation during the load drops was measured with a capacitive transducer, the plates of which were mounted on opposite sides of the grooved section of the crystal. The mass of each plate assembly was 8.75 g, and therefore too small to have any influence on the dynamics of the relaxation process. For some experiments, a plate was mounted to form a capacitor with the $\{\bar{2}\bar{1}0\}$ surface at the lower side of the grooved section of the grounded crystal. Both capacitive transducers have given the same results.

The dynamic load changes during an abrupt elongation were measured with a PZT-4[14] annular ceramic transducer mounted in the lowest universal head. This was calibrated at 4.2 °K against the proving ring by measuring the voltage change for a given load increment or decrement with a vibrating capacitive electrometer.

The outputs from the strain-gauge bridge and differential transformer of the proving ring were chart recorded. The output from the piezoelectric transducer was displayed with the upper beam of an oscillograph and, for each record, the simultaneous output from the capacitive transducer was displayed with the lower beam at the same sweep rate. This proved to be most important because it allowed changes in stress to be correlated with the elongation-time records.

D. Surface topography and etch pits

After their removal from the cryostat, the $\{\bar{2}\bar{1}0\}$ surfaces of the crystals were examined with the optical microscope and the widths of the narrow slip bands measured on both sides with an eyepiece micrometer. The normal displacement of the surface across the bands was determined, again on both sides of the crystal, with the interference microscope from the lateral displacement of thallium light fringes. From the measurements, the plastic shear strain within the slip bands was calculated. Uranium-oxide-preshadowed carbon replicas were made from the $\{\bar{2}\bar{1}0\}$ surfaces.[15] Measurements of the widths and distributions of the individual slip terraces were made on electron micrographs of the replicas. From the results, the numbers and distributions of the dislocations passing through the surfaces were determined. The numbers and distributions of the dislocations retained within the crystals were determined by Hobgood and Mitchell[16] with the etch-pit method.[17] For this work, the crystals were sectioned on $\{1\bar{1}\bar{1}\}$ planes passing through the slip bands.

III. EXPERIMENTAL RESULTS

A. Load-elongation curves

All the crystals were strained at a cross-head speed of 8.33×10^{-5} cm sec^{-1}. In the first series of measurements, the absolute value of the axial load was measured continuously with the strain-gauge transducer of the proving ring. Beyond the

yield point, the load-time curves have regular successive serrations corresponding to abrupt elongations which are initiated from a very nearly constant load level. Two successive load drops are shown in Fig. 1. The constancy of the load over long segments preceding A and following H shows that there is no creep relaxation either within the crystal or at the grips at 4.2 °K. The abrupt elongations were initiated at a resolved shear stress on the $\{\bar{1}\bar{1}1\}\langle 101\rangle$ glide system of 3.01 ± 0.05 kg mm^{-2}. The elongations were determined from the product of the time for elastic recovery from D to the same load level as C and the cross-head speed. For the system including the proving ring, the mean value of the elongation per event was 6.5 ± 0.5 μm. The same mean value was obtained with the differential-transformer transducer. When the harder elastic system was used for the time-resolution work in the second series of measurements of Sec. III B, the mean value for the elongation per event was found to be 4.4 ± 0.5 μm.

B. Time resolution of relaxation events

The plastic elongation-time and load-time records made with the capacitive and piezoelectric transducers for the system with the proving ring were not reproducible due to fluctuations caused by mechanical oscillations. The dynamical characteristics of the mechanical system were analyzed both theoretically and with an electrical-analog system.[18] Following this, the proving ring was eliminated and the system was redesigned to minimize the reflection of stress pulses between the upper end of the crystal and the lower termination of the pull tube. A typical record obtained with the new system is shown in Fig. 2.

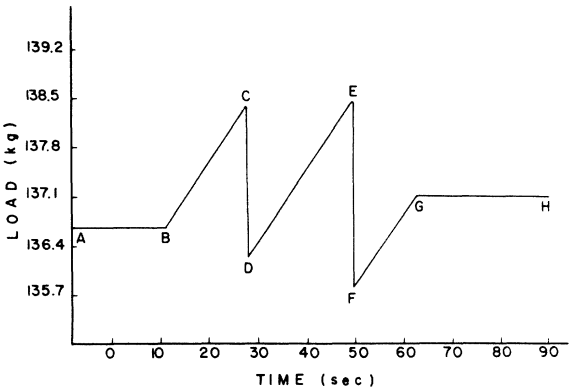

FIG. 1. Tracing of section of load-time chart record showing constant load over segments AB and GH with cross-head stationary, elastic elongation over BC and DE to the yield points at C and E, and load drops CD and EF due to the abrupt elongations. The maximum stress which the crystals would sustain was remarkably constant.

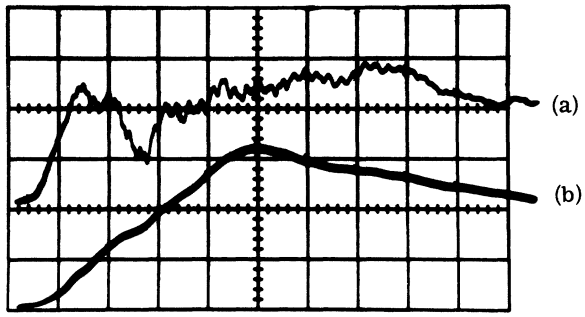

FIG. 2. Simultaneous load-time (upper curve A) and elongation-time (lower curve B) records obtained with piezoelectric and capacitive transducers. On vertical scale, 1 division equals 0.33 kg force and 1 division equals 1.5 μm. On horizontal time scale, 1 division equals 100 μsec.

The lower elongation-time curve shows that, after an initial period of 30 μsec during which a steady state is established, elongation proceeds at a constant average rate of 1.1 cm sec^{-1} for 400 μsec. The upper load-time record shows that the load at the position of the transducer drops by 0.76 kg during the initial 30-μsec interval and then remains constant for 400 μsec. This corresponds to a drop in the tensile stress for this crystal of 0.05 kg mm^{-2}. The mean values of these quantities from 47 records obtained with six crystals are 1.1 ± 0.1 cm sec^{-1} and 0.05 ± 0.01 kg mm^{-2}. All the records gave the same values of 30 and 400 μsec for the initial interval and the duration of the event.

C. Surface topography and etch pits

The study of the $\{\bar{2}\bar{1}0\}$ surfaces with the optical microscope showed that the elongation increments result from the introduction of narrow slip bands of the type previously studied in crystals deformed at room temperature.[11,12,19] With these accurately oriented crystals, there were no slip traces on the $\{1\bar{2}\bar{1}\}$ surfaces which contain the slip vector. The widths of the slip bands on the opposite $\{\bar{2}\bar{1}0\}$ surfaces were always very nearly equal and either 47 ± 10 μm or a multiple of this. The interferograms showed that the mean surface slope was constant across the bands and the same on opposite $\{\bar{2}\bar{1}0\}$ surfaces. The mean plastic shear strain was calculated from measurements of the widths and integrated step heights on both surfaces for a large number of bands in the six crystals deformed with the hard system and found to have an over-all mean value of $11° \pm 2°$. The mean integrated shear displacement across the 47-μm-wide bands was found to be 5.7 μm, in agreement with the mean elongation determined from the load-elongation curves. The quantitative measurements show that the wider bands arise from a number of successive

adjacent events, each producing nearly the same elongation increment.

The detailed structure of the slip bands was determined by replica electron-microscopy[20] and etch-pit methods.[16] The electron micrographs of the replicas show that the slip terraces are arranged in clusters with an average of 20 clusters within the 47-μm bandwidth. The mean width of the bands normal to the $\{\bar{1}\bar{1}1\}$ glide planes was 30 μm so that the mean separation of the glide planes passing through the centers of the clusters was 1.5 μm. The density of the shadowing deposit of uranium oxide on the individual slip terraces was not constant so that they cannot result from slip on single atomic planes.

The etch-pit work on $\{1\bar{1}\bar{1}\}$ sections has established that the long-range dislocations within the slip bands are in near-edge orientations. Near the edges of the slip bands, arrays of light and dark pits[17,21] corresponding to piled-up positive and negative dislocations are often observed on adjacent active glide planes separated by about 1.5 μm. This would correspond with the 1.5-μm spacing of the clusters of glide planes seen in the replicas.[20] This suggests that the clusters of glide planes are activated in pairs with the positive near-edge orientation dislocations moving on one cluster and the negative dislocations moving on the adjacent cluster.[22]

The mean density of long-range primary dislocations within the bands, projected on the $\{1\bar{2}\bar{1}\}$ surface was 1.3×10^{7} cm^{-2}. The area of the slip band projected on this surface is $0.43\times47\times10^{-4}$ cm^2 so that the total number of dislocations retained within a slip band after an event is 2.6×10^{4}. Since there is a uniform average distribution of these dislocations across the glide planes, the motion of each dislocation from the surfaces of the crystal will produce a mean displacement of $\frac{1}{2}b = 1.29\times10^{-8}$ cm. The total shear displacement due to the motion of these dislocations will therefore be 3.4 μm. The mean elongation per event from the load-elongation curves is 4.4 μm. This corresponds to a shear displacement of $4.4/\cos 39°14' = 5.7$ μm. We have therefore to account for a shear displacement of $5.7-3.4=2.3$ μm with dislocations which effectively cross the glide planes from one $\{\bar{2}\bar{1}0\}$ surface to the other. Since these produce a displacement b, the number is $2.3\times10^{-4}/2.57\times10^{-8}=9.1\times10^{3}$. This leads to the conclusion that a total number of 3.5×10^{4} dislocations is involved in the formation of a slip band. Of these, about one quarter or 9.1×10^{3} dislocations effectively cross the glide planes while approximately three-quarters or 2.6×10^{4} dislocations are retained within the slip bands as a uniform distribution on the glide planes. Since there are 10 pairs of clusters, the number of dislocations involved in the activation of each pair is 3500. Of these, 2600 are retained within the crystals and 900 cross the glide planes from one $\{\bar{2}\bar{1}0\}$ surface to the opposite one.

D. Experimental value for nv

These results have been used to establish the model of the relaxation process which is needed before the average velocity of the dislocations can be derived from the rate of elongation.[22] Without the introduction of a model, it is, however, possible to calculate the product of the number n of moving dislocations and their average velocity v in the steady state from the rate of elongation. The rate of elongation is given by the expression $dl/dt=\alpha bnv/s$,[23] where $\alpha=\cos 39°14'$ and $s=0.43/\sin 39°14'$ is the length of the trace of the glide plane in the $\{1\bar{2}\bar{1}\}$ surface. Since $dl/dt=1.1$ cm sec^{-1}, $nv=3.76\times10^{7}$ cm sec^{-1}. This is a reproducible experimental result characterizing the relaxation process in this system.

IV. DISCUSSION

A. Macroscopic features of the relaxation process

The tensile system has a number of elements with different masses and elastic constants which determine its mechanical properties including the normal modes of oscillation[18] and the elastic strain energy stored at the yield point. These elements are (i) the outer tube which is in compression, (ii) the crystal, with the upper and lower universal heads in tension, (iii) the axial pull tube and third universal head in tension, and (iv) the steel block replacing the Instron load cell. There are three important elastic discontinuities in this system: (i) at the interface between the crystal with the lower universal head and the compression tube; (ii) at the interface between the crystal with the upper universal head and the pull tube, and (iii) at the interface between the pull tube with the third universal head and the effectively rigid block at a distance of 101 cm from the site of relaxation. The amplitude reflection coefficients for stress waves at interfaces (i) and (iii) are greater than 0.9, so that the effective mechanical system during an abrupt relaxation consists of the crystal with the upper and lower universal heads, the interface (ii) and the pull tube.

The crystal and the two universal heads participate in high-frequency mechanical oscillations when the state of stress at the yield point is relaxed by an abrupt local elongation near the center of the crystal. The periodic stresses due to the oscillations are superimposed on the applied stress in the crystal and the resultant stresses during the tensile half-cycles cause successive secondary relaxations. The oscillations have been reduced to an ineffective level by minimizing the amplitude reflection coefficient R for the stress pulses pro-

duced by the elongation at the interface (ii). By reducing the dimensions of the upper universal head and the cross-sectional area of the pull tube as far as possible consistent with adequate mechanical strength, a value of $R = 0.3$ was achieved. This approaches the mechanical impedance-matching condition, $A_1 Z_1 = A_2 Z_2$, where A_1, A_2 and Z_1, Z_2 are the areas and impedances of the elements on either side of the interface. These important features of the design of the tensile system have permitted the detailed study of the characteristic properties of the individual relaxation events.

The abrupt relaxations result from shear displacements on $\{\bar{1}\bar{1}1\}$ planes within a narrow slip band about 47-μm wide, located near the center of the crystal. The accompanying axial elongation causes compressive stress waves to propagate outwards in opposite directions. The front of the downward propagating wave in the crystal reaches the lower discontinuity (i) and is reflected as a compressive wave with an amplitude reflection coefficient of about 0.9, about 10 μsec after the initiation of relaxation. After the passage through the site of relaxation of the stress wave reflected at (i), the crystal on the lower side of the slip band is stationary, because of the superposition of nearly equal and opposite particle velocities. Two compressive stress waves are therefore propagated up the pull tube with a time delay of about 20 μsec between the wave fronts. The experimental observations show that they are reflected as compressive stress waves at the upper discontinuity (iii) and return to the site of relaxation 400 μsec after the initiation of the process. This is in quantitative agreement with the transit time for a longitudinal sound wave up the crystal to (iii) and back.

The load-time curve A of Fig. 2 shows that 30 μsec after the initiation of relaxation, and following the upward propagation of the two stress waves, the tensile stress in the crystal falls by $\Delta\sigma_{33}^c = 0.05$ kg mm^{-2} and thereafter the mean stress in the crystal, σ_{33}^c remains constant. The initial stress is $\sigma_{33}^0 = 6.14$ kg mm^{-2} so that the stress in the crystal after the initiation of relaxation is $\sigma_{33}^c = \sigma_{33}^0 - \Delta\sigma_{33}^c = 6.09$ kg mm^{-2} (x_{33} lies along the $[\bar{1}2\bar{5}]$ axis of the crystal and the axis of the pull tube).

The stress in the crystal is determined by the dynamical equation of motion of a stress wave,[24]

$$\sigma_{33}^c = \sigma_{33}^0 - Z^c\left(\frac{du}{dt}\right) \quad \text{or} \quad \Delta\sigma_{33}^c = \sigma_{33}^0 - \sigma_{33}^c = Z^c\left(\frac{du}{dt}\right), \tag{1}$$

where $Z^c = \rho c$ (ρ is the density and c is the velocity of longitudinal sound waves) is the characteristic impedance of the crystal and du/dt is the particle velocity of the moving half of the crystal. Curve B of Fig. 2 shows that this particle velocity on the upper side of the developing slip band has a constant mean value of 1.1 cm sec^{-1}. This is determined by the product of the number and the velocity of the moving dislocations. Because of continuity, in the interval $30 < t < 200$ μsec this must so be the upward velocity of the pull tube behind the stress fronts. We have $Z^{pt}(du/dt)^{pt} = \Delta\sigma_{33}^{pt}$, where $Z^{pt} = 4.1 \times 10^6$ g cm^{-2} sec^{-1} and $du/dt = 1.1$ cm sec^{-1}. With these values, $\Delta\sigma_{33}^{pt} = 4.5 \times 10^6$ dyn cm^{-2} $= 0.046$ kg mm^{-2}. The stress difference required to establish the particle velocity in the crystal is then given by $\Delta\sigma_{33}^c = Z^c \Delta\sigma_{33}^{pt}/TZ^{pt}$, where T is the transmission coefficient, 0.7 at the interface (ii). $Z^c = 2.73 \times 10^6$ g cm^{-2} sec^{-1} so that $\Delta\sigma_{33}^c = 0.044$ kg mm^{-2}. This is as close to the measured value of 0.05 kg mm^{-2} as would be anticipated from the experimental error and the simplifications inherent in the model and the analysis. The agreement establishes the self-consistency of the measurements which have been made with the piezoelectric and capacitive transducers.

The behavior of the crystal during an abrupt load drop is thus determined by the dynamical characteristics of the mechanical system. The constant rate of axial elongation at the slip band of 1.1 cm sec^{-1} maintains a constant particle velocity in the steady state during the 400-μsec transit time of the stress pulses. Elongation ceases when the stress pulses return and pass through the slip band, reducing the tensile stress by a further 0.05 kg mm^{-2} so that elongation occurs only over a very small range of shear stresses.

The physical basis for the compensating mechanism which suppresses the small fluctuations in the elongation rate seen in Fig. 2 can now be understood. A reduction in the rate produces an immediate reduction in the local particle velocity du/dt of the crystal above the relaxation site. Since $\Delta\sigma_{33}^c/(du/dt) = Z^c = \text{const}$, $\Delta\sigma_{33}^c$ must immediately decrease and, from Eq. (1), σ_{33}^c and the resolved shear stress on the glide planes within the slip band must rise. This produces an increment in the product nv and the elongation rate will therefore increase until the steady-state value is reestablished. The correlation between decreases in the rate of elongation and decreases in $\Delta\sigma_{33}^c$ is clearly seen in curves A and B of Fig. 2.

B. Energetic aspects of the relaxation process

The macroscopic features of the relaxation process can also be considered from an energetic viewpoint. For the crystal, the elastic-strain energy density at the yield point is given by $w = \frac{1}{2} s_{33} (\sigma_{33}^0)^2$. For a Cu-10.5-at.%-Al crystal with a $[\bar{1}2\bar{5}]$ axis at 4.2 °K, s_{33} has an estimated value of 1.11×10^{-12} dyn^{-1} cm^2. This is based on an accurate calculation of s_{33} at room temperature from the measured elastic constants[25] and an estimate of the change in s_{33} between room temperature and 4.2 °K. At 4.2 °K, σ_{33}^0 is 6.14 kg mm^{-2}, so w^c

$= 2.0 \times 10^5$ erg cm^{-3}. For the stainless-steel pull tube, $w^{pt} = 5.1 \times 10^5$ erg cm^{-3}. The passage of the two stress waves reduces the tensile stress by 0.044 kg mm^{-2} in the crystal and by 0.046 kg mm^{-2} in the pull tube. The elastic-strain energy densities are therefore reduced by $\Delta w^c = -2.8 \times 10^3$ erg cm^{-3} and $\Delta w^{pt} = -0.99 \times 10^3$ erg cm^{-3}. During the steady-state relaxation ($t > 30$ μsec), the potential energy of the system is decreased by the propagation of the stress waves up the pull tube at the rate of $\Delta W^{pt}/\Delta t = -cA\Delta w^{pt} = -1.2 \times 10^8$ erg sec^{-1}, where c is the velocity of sound in stainless steel (5.17×10^5 cm sec^{-1} at 4.2 °K) and A is the cross-sectional area of the pull tube (0.24 cm^2). The small change due to the propagation of the stress wave in the outer compression tube is not included.

We now consider the possible processes whereby this decrease in the potential energy of the system is converted into other forms of energy. For $t > 30$ μsec, the sections of the crystal and pull tube between the slip band and the wave fronts are moving with a constant upward velocity of 1.1 cm sec^{-1}. A small fraction of the potential energy of the pull tube will therefore be converted into kinetic energy at the rate of $\Delta K/\Delta t = -\frac{1}{2}cA\rho(du/dt)^2 = 5.9 \times 10^5$ erg sec^{-1}. A negligible amount is converted into thermal energy in the volume of the crystal and the pull tube during the adiabatic propagation of the stress waves. The experimental observations show that a number of dislocations equal to 3.5×10^4 is introduced with an energy per unit length of 3.96×10^{-4} erg cm^{-1} and an individual length of 0.43 cm. For a uniform rate of introduction over 400 μsec, this gives a negligible rate of conversion of 1.5×10^4 erg sec^{-1}. Most of the potential energy must therefore be converted into thermal energy at the slip band at the rate of 1.2×10^8 erg sec^{-1} through work done by the dislocations against the effective frictional forces acting on them. This conversion occurs in a band with a width of 30 μm normal to the glide planes. The order of magnitude of the width of the region experiencing a temperature change during the 400-μsec process is given by $\Delta x = 2(4\alpha t)^{1/2}$. With $\alpha = 20$ cm^2 sec^{-1}, estimated from specific-heat and thermal-conductivity data,[26] this gives $\Delta x = 0.36$ cm. The conversion of the potential energy into thermal energy within this volume leads to a temperature increase of the order of 13 °K which corresponds to a temperature of 17 °K within the slip band.

C. Microscopic mechanism of the relaxation process

We next consider the relaxation process in terms of the generation and migration of dislocations. The detailed mechanism, which will be presented in a separate paper,[22] will be summarized here and the model will be used in Sec. IV D to arrive at an estimate of the average velocity with which the dislocations move during the abrupt elongations. When the axial tensile stress reaches a value of 6.14 kg mm^{-2} corresponding to a shear stress of 3.01 kg mm^{-2} on the $\{\bar{1}\bar{1}1\}\langle 101\rangle$ glide system, relaxation is initiated by the activation of a dislocation source which emits rapidly expanding loops. When segments of these loops reach either or both of the opposite $\{\bar{2}\bar{1}0\}$ surfaces, broad internal stress maxima are developed ahead of the moving dislocations which are superimposed additively on the applied stress at the acute angles between the glide plane and the surfaces.[27] Many sources at or near the $\{\bar{2}\bar{1}0\}$ surfaces are now activated in one or both of these regions. In either case, a self-sustaining unit relaxation process is rapidly established in which dislocations in near edge orientations with Burgers vectors of opposite sign move in opposite directions on two adjacent clusters of glide planes with centers separated by about 1.5 μm. There is no long-range stress field associated with such a distribution of dislocations. The long-range motion of the dislocations on the first pair of clusters results in a local generation of thermal energy by work done against frictional forces. This produces a symmetrical temperature distribution on either side of the pair of clusters. The etch-pit studies show that the long-range motion of the dislocations is terminated by the activation of the $\{\bar{1}1\bar{1}\}\langle\bar{1}\bar{1}0\rangle$ and $\{111\}\langle 01\bar{1}\rangle$ glide systems. This introduces forests of secondary dislocations which impede the motion of the primary dislocations by combining with them to produce high densities of sessile segments.[28] When this happens, the rate of elongation is reduced and the local shear stress rises. Since the resolved shear stress for the activation of sources decreases with increasing temperature,[9,29] new pairs of clusters are activated in the higher-temperature region on either side of the first cluster and beyond the range of the secondary dislocations. These processes continue with widening of the slip band until the return of the reflected stress pulses. Motion on the outer activated clusters then ceases because the primary dislocations are unable to overcome the frictional stresses under the action of the lower shear stress. The temperature falls and the stress required for the activation of new sources increases. Activation cannot now occur until the shear stress is increased by the relatively slow motion of the cross-head of the tensile machine. During this period, the slip band is inactive and a new band is usually introduced at another site in the crystal.

D. Calculation of the average dislocation velocity

We now develop a quantitative discussion which is consistent with the model for the relaxation process outlined in the previous section. Averaging is used to avoid the introduction of unobservable

details of the process. We have seen that elongation proceeds at a constant rate, dl/dt for t seconds, and that during this interval, N dislocations are introduced on m pairs of clusters of primary glide planes. The total number of dislocations in each pair of clusters will be N/m and the clusters will be active for t/m seconds. The long-range displacement of these dislocations is responsible for the observed elongation. We now assume that the dislocations are introduced continuously at a constant average rate of N/t sec^{-1}, motion on the succeeding pair of clusters beginning when motion on the preceding pair ceases through secondary activation. The average number of moving dislocations in each pair of clusters during the interval t/m seconds will therefore be $N/2m$. We further assume that these dislocations have the average velocity, v, during the whole period of their motion. The rate of elongation is then independent of the displacement of the dislocations across the glide planes since, for one dislocation, $dl/dt = (\alpha bd/s)/(d/v) = \alpha bv/s$, where α is a geometrical factor equal to $\cos 39°14'$, d is the displacement across the glide plane, and s the length of the trace of the glide plane in the $\{1\bar{2}\bar{1}\}$ surface. For $N/2m$ dislocations, we therefore have $dl/dt = \alpha bvN/2ms$. From the experimental measurements, $(N/2m)v = 3.76\times10^{7}$ cm sec^{-1}. With $N = 3.5\times10^{4}$ and $m = 10$, we obtain for the average velocity, v the value of 2.1×10^{4} cm sec^{-1}. The steady state is established within 30 μsec of the initiation of relaxation. The dislocations therefore move with this average velocity at the steady-state temperature of about 17 °K and at a resolved shear stress of 2.98 kg mm^{-2}.

We have seen that the rate of conversion of potential energy into thermal energy during the formation of a slip band is 1.2×10^{8} erg sec^{-1}. This rate is given by $\Delta W/\Delta t = n\sigma bvx = nBv^{2}x$ in terms of the nv product and the velocity v, where B is the velocity damping constant and $x = 0.43$ cm is the length of the edge dislocations in the crystal. With the measured values of $\Delta W/\Delta t$ and nv, we obtain $Bv = 7.6 \pm 0.7$ dyne cm^{-1}. This is independent of the model and microscopic mechanism used to calculate the average velocity of 2.1×10^{4} cm sec^{-1}. With this value, we find $B = 3.6\times10^{-4}$ dyn sec cm^{-2}. This is approximately an order of magnitude higher than that obtained by extrapolating the measurements of Jassby and Vreeland[29] with pure copper crystals to 17 °K. The increase is probably to be attributed to the greater frictional resistance opposing the motion of the dislocations in the alloy crystals.

E. Nature of the instability of the system

The experimental observations and numerical calculations which lead to the model of the relaxation process[22] support the hypothesis that the instability of the system at the yield point has its origin in the generation of dislocations at a rapidly increasing number of sources within each successively activated pair of clusters of glide planes. Although the model is different, this conclusion on the nature of the instability is so far consistent with those of Seeger,[3] Haasen,[4] and Kamada.[5]

During the formation of a slip band, part of the potential energy of the elastically strained system is converted into thermal energy as work is done against frictional forces opposing the motion. Since the resolved shear stress at the yield point, required for the activation of dislocation sources, decreases with increasing temperature, this further increases the probability for the activation of sources by the resultant stresses.

The experimental observations demonstrate conclusively that a dynamically stable steady state is established 30 μsec after the initiation of relaxation and that elongation then proceeds at a constant rate of 1.1 cm sec^{-1} for a further interval of 370 μsec when it is terminated by a further decrease of 0.024 kg mm^{-2} in the resolved shear stress on the glide planes. The local temperature at the slip band in the steady state is estimated to be 17 °K.

The discussion of Sec. IV A shows that the relaxing system in the steady state is stable against fluctuations in the rate of elongation and that the dynamic stability appears to be determined by the mechanical condition, $\Delta\sigma_{33}^{c}/(du/dt) = Z^{c} = \text{const}$, which requires the observed increase in $\Delta\sigma_{33}^{c}$ when the rate of elongation increases and vice versa. Through this condition, the system is also dynamically stable against temperature fluctuations which accompany or produce fluctuations in the rate of elongation in the steady state and cause fluctuations in the nv product.

We therefore conclude that the discussion of Basinski[6,7] can only be relevant to the first 30 μsec of the 400-μsec relaxation process in this system. Within this interval, it is not at the present time possible to maintain that the instability is entirely of thermal origin. Although the resolved shear stress for the activation of sources falls continuously above 4.2 °K, thermally activated creep at stresses close to the yield stress is not observed below 8 °K.[30] In the transition regime below 8 °K where relaxation is initiated, it therefore appears that the internal stresses associated with the moving dislocations play a more important role than the increase in temperature in producing a rapid increase in the number of sources so that the instability is probably of mechanical rather than of thermal origin.

ACKNOWLEDGMENTS

We wish to thank J.S. Ahearn, Jr., H. McD.

Hobgood, W. E. Nixon, and D. A. Taliaferro for assistance with the low-temperature work. We also wish to thank Dr. J. W. Beams, Dr. R. V. Coleman, Dr. B. S. Deaver, and Dr. G. B. Hess for the loan of electronic and recording equipment. We are grateful to Mr. Henry Zumbrum of the Morehouse Instrument Co., York, Pa. for providing us with two high-quality proving rings. The support of this work by the U.S. Atomic Energy Commission is very gratefully acknowledged.

---

†Research supported by the U. S. Atomic Energy Commission under Contract No. AT-(40-1)-3808.

*Present address: Department of Physics, University of Illinois, Champaign-Urbana, Ill.

[1]T. H. Blewitt, R. R. Coltman, and J. K. Redman, J. Appl. Phys. 28, 651 (1957).

[2]T. H. Blewitt, R. R. Coltman, R. E. Jamison, and J. K. Redman, J. Nucl. Mat. 2, 277 (1960).

[3]A. Seeger, in *Dislocations and Mechanical Properties of Crystals*, edited by J. C. Fisher, W. G. Johnston, R. Thomson, and T. Vreeland, Jr. (Wiley, New York, 1957), p. 206.

[4]P. Haasen, Philos. Mag. 3, 384 (1958).

[5]K. Kamada, Trans. Jap. Inst. Met. 7, 15 (1966).

[6]Z. S. Basinski, Proc. R. Soc. A 240, 229 (1957).

[7]Z. S. Basinski, Aust. J. Phys. 13, 354 (1960).

[8]J. C. Erdmann and J. A. Jahoda, J. Appl. Phys. 39, 2793 (1968).

[9]K. Kamada, I. Yoshizawa, and T. Chihaya, Trans. Jap. Inst. Met. 9, 443 (1968).

[10]K. Kamada and I. Yoshizawa, J. Phys. Soc. Jap. 31, 1056 (1971).

[11]J. W. Mitchell, J. C. Chevrier, B. J. Hockey, and J. P. Monaghan, Jr., Can. J. Phys. 45, 453 (1967).

[12]J. S. Ahearn, Jr., H. McD. Hobgood, and J. W. Mitchell, *Second International Conference on the Strength of Metals and Alloys* (American Society of Metals, Cleveland, Ohio, 1970), p. 416.

[13]J. S. Ahearn, Jr., J. P. Monaghan, Jr., and J. W. Mitchell, Rev. Sci. Instrum. 41, 1853 (1970).

[14]D. A. Berlincourt, D. R. Curran, and H. Jaffe, in *Physical Acoustics*, edited by W. P. Mason (Academic, New York, 1964), Vol. 1 A, p. 336.

[15]J. S. Ahearn and J. W. Mitchell, Rev. Sci. Instrum. 42, 94 (1971).

[16]H. McD. Hobgood and J. W. Mitchell (unpublished).

[17]B. J. Hockey and J. W. Mitchell, Philos. Mag. 26, 409 (1972).

[18]R. B. Schwarz, Ph.D. thesis (University of Virginia, 1972) (unpublished).

[19]J. W. Mitchell, J. S. Ahearn, Jr., B. J. Hockey, J. P. Monaghan, Jr., and R. K. Wild, Trans. Jap. Inst. Met. Suppl. 9, 769 (1968).

[20]W. E. Nixon and J. W. Mitchell (unpublished).

[21]J. D. Livingston, in *Direct Observations of Imperfections in Crystals*, edited by J. B. Newkirk and J. H. Wernick (Interscience, New York, 1962), p. 115.

[22]J. S. Ahearn, Jr., H. McD. Hobgood, J. W. Mitchell, W. E. Nixon, R. B. Schwarz, and D. A. Taliaferro (unpublished).

[23]F. Seitz and T. A. Read, J. Appl. Phys. 12, 470 (1941).

[24]H. Kolsky, *Stress Waves in Solids* (Clarendon, Oxford, 1953), p. 43.

[25]L. S. Cain and J. F. Thomas, Jr., Phys. Rev. B 4, 4245 (1971).

[26]D. R. Zrudsky, W. G. Delinger, W. R. Savage, and J. W. Schweitzer, Phys. Rev. B 3, 3025 (1971); P. Charsley and J. A. M. Salter, Phys. Status Solidi 10, 575 (1965); P. Charsley, J. A. M. Salter, and A. D. W. Leaver, Phys. Status Solidi 25, 531 (1968); M. A. Mitchell, P. G. Klemens, and C. A. Reynolds, Phys. Rev. B 3, 1119 (1971).

[27]D. A. Taliaferro, L. F. Henry, III, and J. W. Mitchell, J. Appl. Phys. 45, 519 (1974).

[28]Z. S. Basinski, Discuss. Faraday Soc. 38, 93 (1964).

[29]K. M. Jassby and T. Vreeland, Jr., Philos. Mag. 21, 1147 (1970).

[30]R. B. Schwarz and J. W. Mitchell (unpublished).